

On the excitation and damping of Alfvénic waves throughout the solar atmosphere:

Insights from chromospheric power spectra



R J Morton¹, G Verth², A Hillier³ & R Erdélyi²
¹Northumbria University, UK, ²Sheffield University, UK, ³Kyoto University, Japan



Introduction

It has long been proposed that the kinetic energy in stellar convective envelopes is transferred throughout stellar atmosphere via the magnetic field [1]. A number of popular theories assume that the horizontal components of the motion of convective granulation, observed at the solar photospheric surface, excite incompressible MHD transversal (Alfvénic) waves in magnetic flux concentrations [2]. These incompressible motions can either be perpendicular to the constant magnetic surfaces (i.e. kink modes) or perpendicular to the field lines within these surfaces (i.e. torsional Alfvén modes) [3].

More recently, advanced analytical and numerical models have used velocity power spectra estimated from observations of the solar granulation [3-5] as their input spectrum for generating incompressible waves in stellar atmospheres. These models have had some success in generating the necessary non-thermal energy needed for plasma heating in the atmospheric layers and providing the necessary energy flux for accelerating solar winds. However, it was not clear whether the velocity power spectra derived from the horizontal motions were the physically appropriate input for the models. In addition, MHD kink wave energy estimates from observations hint that the chromospheric fine structure [6, 7] exhibits much more energetic motion than the coronal fine structure [8, 9]. However, no attempt has yet been made to demonstrate the transport of kink wave energy between the different atmospheric layers, which is essential for distinguishing between various heating models.

Here, we provide a missing link in this problem by determining chromospheric velocity power spectra from observations. This allows for the comparison of the chromospheric power spectra to other velocity power spectra derived at different altitudes, which reveal the first observational details of kink energy transport through the solar atmosphere.

Observations

The hydrogen alpha (H α) spectral line has proved invaluable for exploration of the magnetically dominated chromosphere [10], in particular for incompressible wave studies. Here we use two H α datasets taken with Rapid Oscillations in the Solar Atmosphere (ROSA - [11]) at the Dunn Solar Telescope at Sacramento Peak, USA. Both datasets are positioned relatively close to disk centre, which implies the line-of-sight (LOS) is almost vertically down into the solar atmosphere.

The datasets were obtained at 15:24-16:35 UT on 22 August 2008 (D1) and 15:41-16:51 UT on 29 September 2010 (D2). Both datasets were taken with a spatial sampling of 0".069/pixel. ROSA obtained images in multiple wavelengths including G-band (4305.5 Å) with a 9 Å width and H α core (6562.8 Å) narrowband (0.25 Å) filters. The post-reconstruction cadence of the G-band, H α time-series are 12.8 s, 6.4 s for D1 and 0.96 s, 7.7 s for D2.

D1 focuses on a region of relatively strong magnetic activity, with the G-band images of the photosphere (Figure 1) revealing underlying magnetic bright points and dark magnetic pores. In contrast, the G-band for the second dataset (D2) reveals only magnetic bright points, suggesting the total magnetic flux underlying the D2 H α region is significantly less than in D1. The affect of the differing magnetic fluxes is reflected in the chromospheric features detected in H α .

We also make use of results obtained from different instruments. The photospheric velocity power spectrum was obtained using the Hinode Solar Optical Telescope (SOT) G-band channel and further details are given in [4]. The data were obtained on the 18 March 2007. The other photospheric power spectra were obtained using the Swedish Solar Telescope and further details are given in [12]. The data were obtained on the 18 June 2006. The coronal velocity power spectrum was obtained using the Coronal Multi-channel Polarimeter (CoMP) and details are given in [13]. The data were obtained on the 30 October 2005.

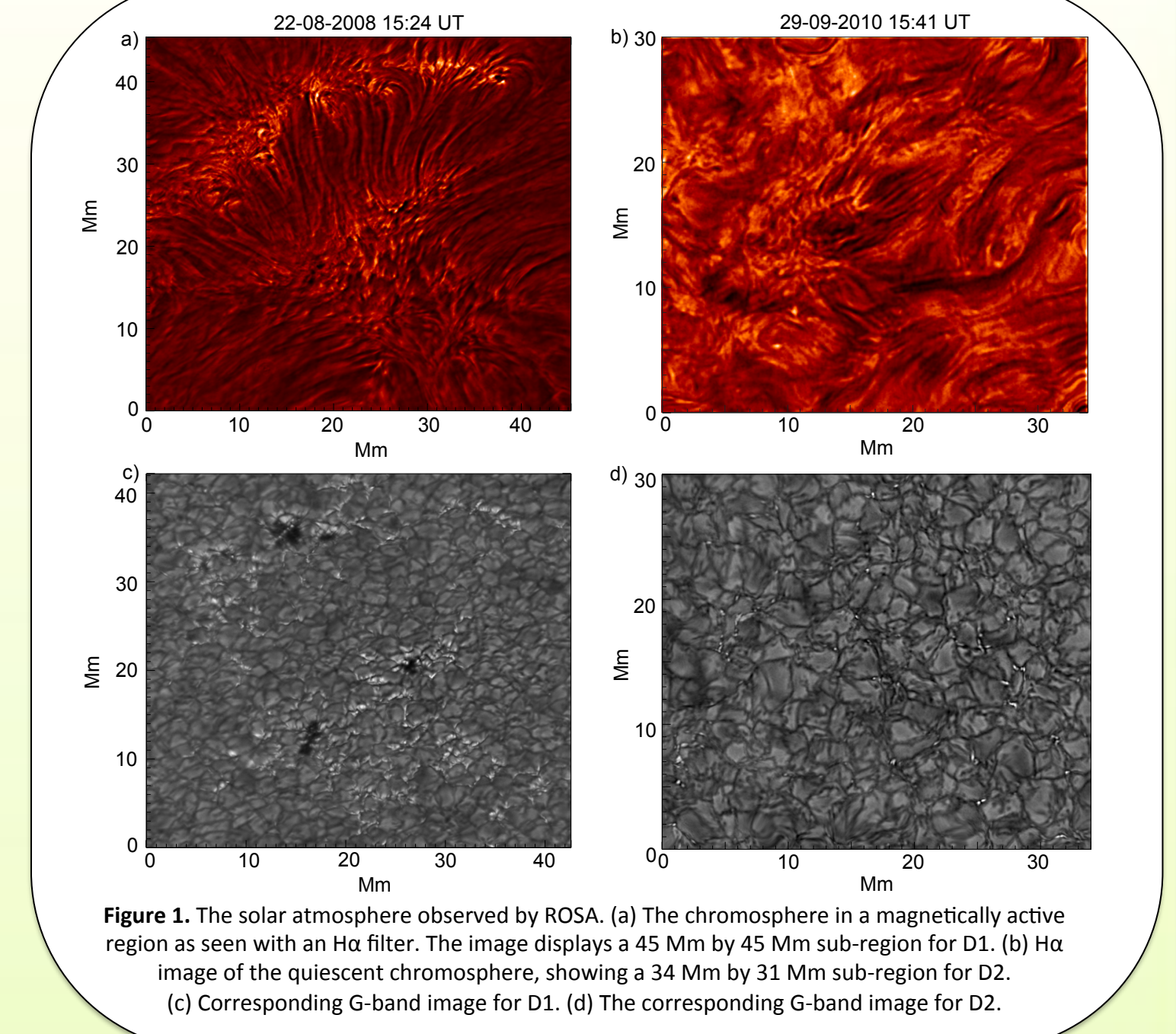


Figure 1. The solar atmosphere observed by ROSA. (a) The chromosphere in a magnetically active region as seen with an H α filter. The image displays a 45 Mm by 45 Mm sub-region for D1. (b) H α image of the quiescent chromosphere, showing a 34 Mm by 31 Mm sub-region for D2. (c) Corresponding G-band image for D1. (d) The corresponding G-band image for D2.

Measured wave properties

On analysing the H α movies of these two regions, the dynamic behaviour of the chromospheric fine structure is evident. Our interest is directed towards the axial transverse displacement of the chromospheric fibrils, which is the unique signature of MHD kink wave motion. The transverse fibril displacements are identified and measured using a semi-automated tracking mechanism [14]. In D1 and D2, a total of 744 and 841 sinusoidal transverse displacements are measured, respectively. Histograms of the periods, transverse amplitudes and velocity amplitudes are given in Figure 2. The previous observations in fibrils [7, 14], off-limb spicules [6, 15] and other small-scale chromospheric features [16] are found to be consistent with the results obtained here.

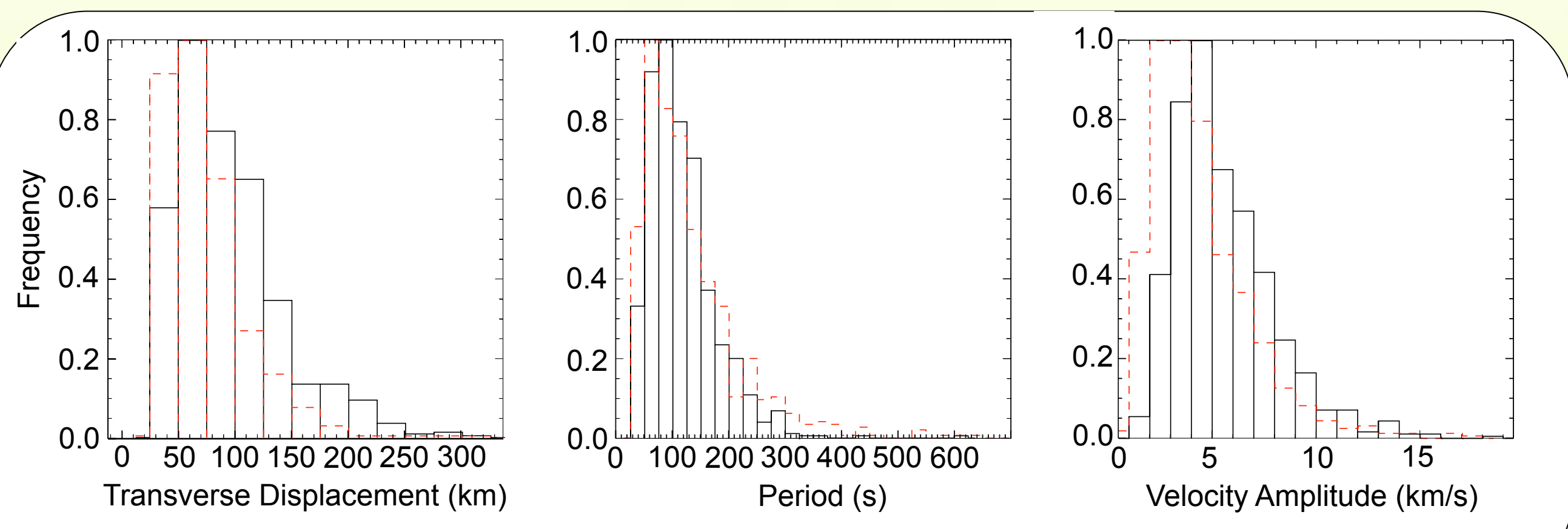


Figure 2. Histograms of measured wave properties from data sets D1 (red) and D2 (black).

Evidence for photospheric excitation

Now, the velocity power (v^2/f) is determined and the data points from the generated PDFs are plotted in Figure 4. In addition, the photospheric velocity power spectra, measured from two different characteristic sets [4, 12] of quiescent photospheric data, are over-plotted. The photospheric results are scaled up by factors of 15-70 for better visualisation, due to the smaller velocity amplitudes in the photosphere. The increase in amplitude from the photosphere to chromosphere is expected because of the increase in Alfvén velocity with height.

The gradient of the chromospheric power spectrum for D1 is relatively flat and does not appear to show a correlation with the photospheric power spectra. The lack of similarity could suggest that photospheric motions are not responsible for the driving of the waves in the active regions. Conversely, the photospheric velocity power spectra are derived for quiescent Sun regions. Photospheric flow measurements [17] show that flows are suppressed as the magnetic activity increases; hence, the photospheric motions in active regions may produce waves with an alternate power spectra.

In contrast to the results for D1, a very good agreement exists between the gradients of the quiescent chromospheric (D2) and photospheric velocity power spectra for waves with $f < 0.01$. The correlation indicates that the horizontal photospheric motions could be responsible for generating the chromospheric dynamics (power spectra for transverse waves in prominences also displays a similar correlation with horizontal photospheric motions [18]). For the higher frequency waves, $f > 0.01$, the chromospheric power spectra suggests there enhanced power over the photospheric spectra.

Further work is required to establish a direct cause and effect relationship between the horizontal motions and the transverse waves observed higher in the solar atmosphere, e.g., via the inclusion of phase spectra.

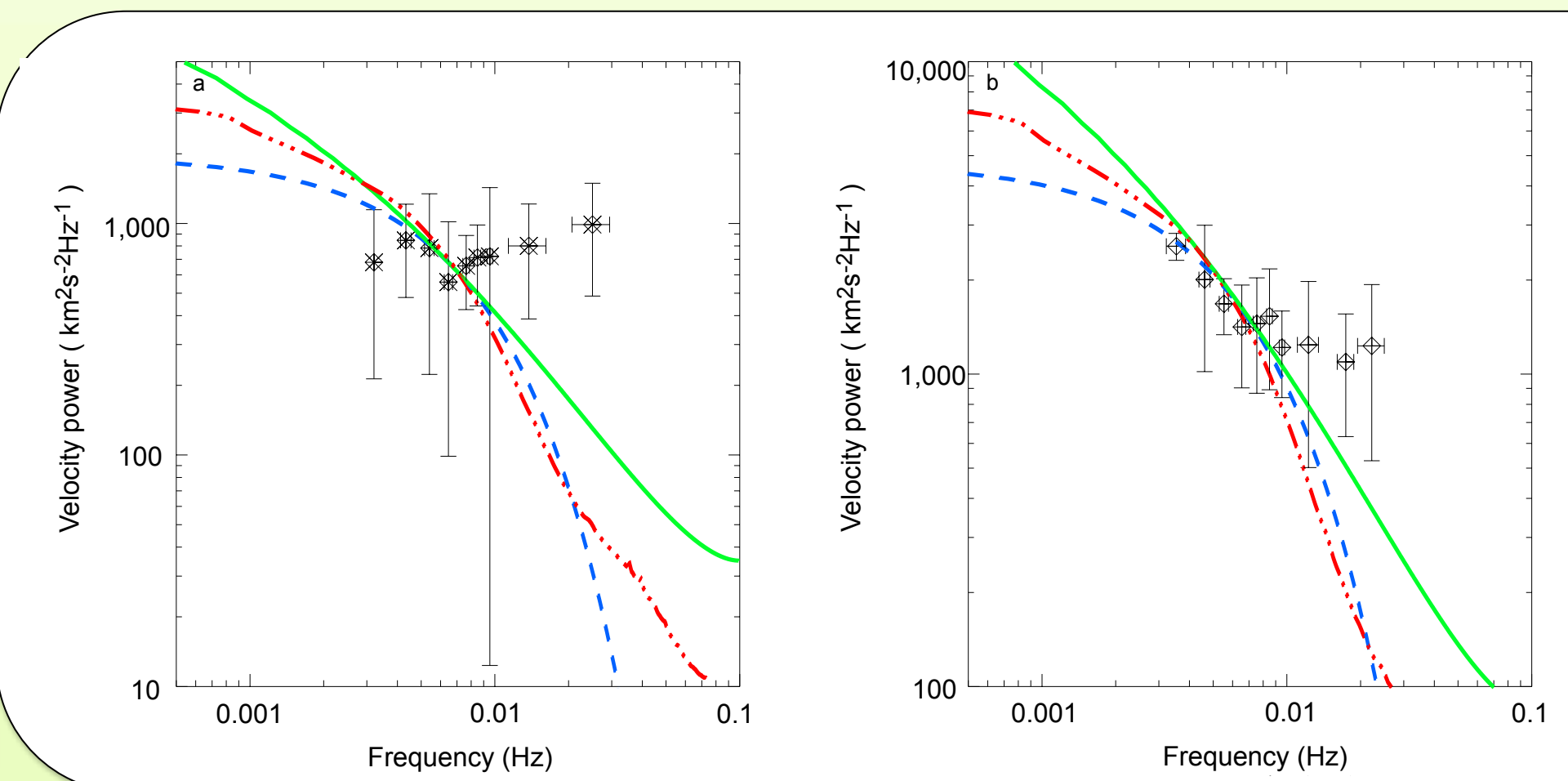


Figure 4. Comparing the power spectra of the photosphere and chromosphere. (a) The figure displays the median velocity power in the chromosphere as a function of frequency for the magnetically active region D1. The velocity power data points are calculated from frequency binned PDFs and the vertical error bars show the standard deviation of the velocity power in the bins. Over-plotted are the photospheric velocity power spectra of horizontal motions; (4) red dash dot, and (12) green solid and blue dash. The photospheric data has been scaled by a constant factor for comparison. (b) Same as (a) but for the quiescent Sun region D2. It is apparent that the gradient of the chromospheric profile from the quiescent Sun (D2) agrees with that from photospheric power spectra.

Conclusions

The results presented here show that the measurement of velocity power spectra provides a powerful and practical mechanism for analysing MHD kink wave propagation through the magnetised solar atmosphere. Comparing the velocity power spectra obtained at different altitudes of the atmosphere allows for the possible signatures of kink wave driving and damping to be observed (as summarised by Figure 6). The picture implied by the observations presented here suggests a qualitative agreement with theoretical expectations for wave propagation through the quiescent solar [3], i.e., magnetic waves are driven by the horizontal motions that propagate into the upper solar atmosphere, with the flow of wave energy hindered by the strong gradients present in the transition region. The intimation of enhanced and frequency-dependent kink wave damping between the chromosphere and corona has potentially important implications for numerous coronal-heating models, which demonstrate that incompressible wave energy is more efficiently converted to heat at higher frequencies.

These observational results do not tell the complete picture though and they raise a number of key questions that need to be answered, e.g., what is the fate of the high-frequency wave energy observed in the chromosphere? What mechanism(s) has led to their decrease in power before they reach the corona? One possible explanation of coronal kink wave damping is through mode conversion to $m=1$ torsional Alfvén waves at resonant magnetic surfaces naturally present across inhomogeneous solar atmospheric waveguides. Such a process could also explain the stronger kink wave damping in the interface layer (the 15-20 Mm region linking between ROSA and CoMP observations). In the lower atmosphere (at heights of less than 10 Mm) it has recently been shown that torsional Alfvén and kink waves are concurrent in spicules [22], providing evidence that mode coupling is potentially already happening at sub-interface region heights. To fully understand the interaction and evolution of these coupled incompressible MHD wave modes in the interface layer between the chromosphere and corona, upcoming missions such as the Interface Region Imaging Spectrometer will be crucial.

Frequency dependence

Figure 3 shows how the measured transverse displacement and velocity amplitude vary as function of period. To provide a fit to the generated data points, we bin the data in the frequency domain and for each frequency bin we take the log of the data and plot a probability density function (PDF). A Gaussian is fit to each PDF and the centroid gives the median log value while the width provides the standard deviation. The data points generated from the PDFs are then fitted with a power law of the form 10^{aP^b} (where P is the period of the wave) and is weighted by the standard deviation of each PDF divided by the square root of the number of elements in each distribution, i.e., the standard error.

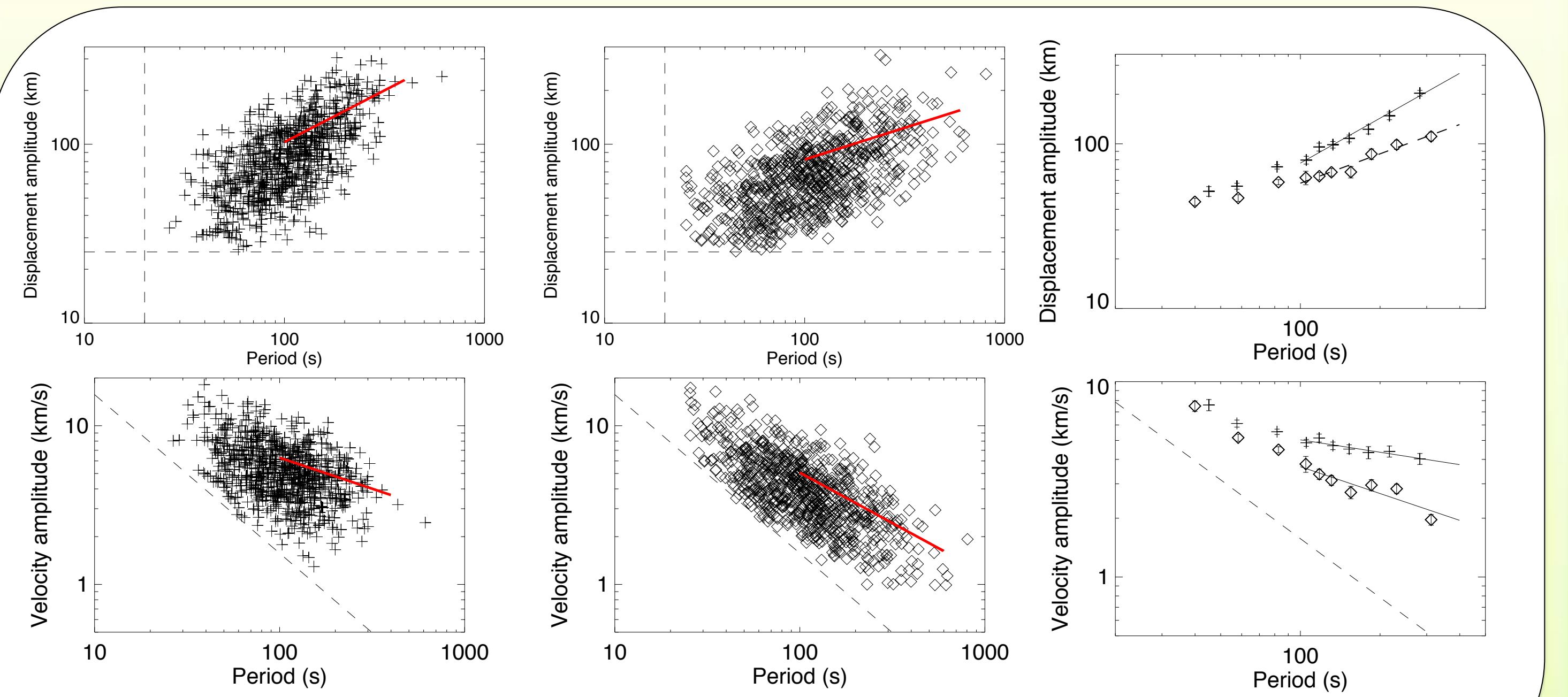


Figure 3. Scatter plots of measured wave properties from data sets D2 (left) and D1 (middle). The red lines are the power law fits to the PDF generated data points. The two right hand panels show the PDF generated data points for D1 (diamonds) and D2 (crosses). The standard error on each point is shown by the error bars. Solid lines are the power law fits.

Evidence for damping in the low corona

Let us now compare the chromospheric power spectrum to those derived for the corona. Figure 5a shows the velocity power measured with CoMP for a coronal loop arcade structure in a quiescent Sun region divided by the fitted power law for the chromospheric velocity power from region D2. The velocity power of the CoMP data is, however, averaged over a distance of 250 Mm along a coronal loop system, where frequency-dependent wave damping has occurred [13, 19]. The input power spectra at the base of the CoMP loop system (at a height of 20 Mm) is determined by exploiting the measured damping rates [19, 20] and also compared with the chromospheric spectrum. A frequency dependent trend is clear and shows an order of magnitude decrease in velocity power for the higher frequency waves ($f > 10$ mHz) relative to the lower frequency waves ($f < 2$ mHz).

In Figure 5b and c, the ratios of velocity amplitudes, the integrated total energy and integrated Poynting flux between the corona and the chromosphere are also shown. These findings come with the following caveat: the spatial sampling (≈ 4.5 Mm) of CoMP means it may not resolve the coronal fine structure adequately. It has been demonstrated the effect of LOS integration on multiple unresolved loops leads to an underestimate of kink wave velocity amplitude [21].

The observed frequency-dependent trends of the quantities in Figure 5 can be explained by frequency-dependent damping. In the case of propagating waves the quality factor is L_D/λ , where L_D is the damping length and λ is the wavelength. Assuming that frequency-dependent damping also occurs in the interface region between ROSA and CoMP observations, we can estimate the interface region damping. Writing $L_D = \alpha/f$, we find $\alpha_{int} \approx 0.1$ provides a reasonable approximation of the change in gradient between ROSA and CoMP velocity power spectra. From the analysis of the damping of propagating coronal kink waves $\alpha_{corona} \approx 1.6$ [19]. It follows that the quality factor in the interface region is about 6% of the estimated coronal damping length. Hence, the observed trend implies that there is much stronger frequency-dependent kink wave damping in the Transition Region and lower corona.

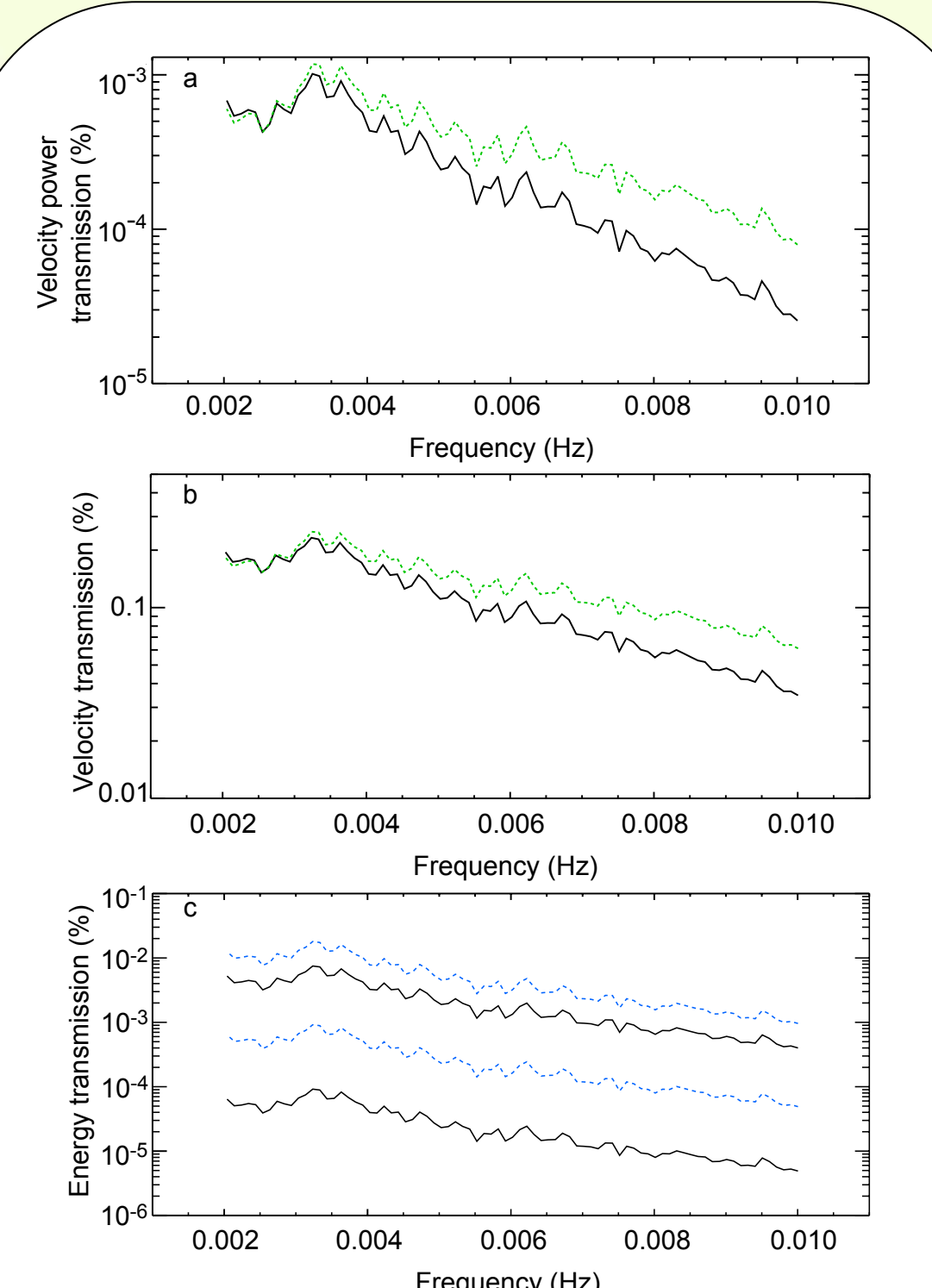


Figure 5. Transmission profiles from the chromosphere to the corona. (a) The ratio of velocity power. (b) The ratio of velocity amplitudes. The solid lines are spatially averaged CoMP measurements. The dashed lines are estimated input power/velocity in the corona at a height of 20 Mm. (c) The ratio of integrated total wave energy (solid lines) and the ratio of integrated Poynting flux (dashed lines). The two lines for each quantity correspond to the maximum and minimum ratios possible, reflecting the uncertainty in known values of plasma parameters.

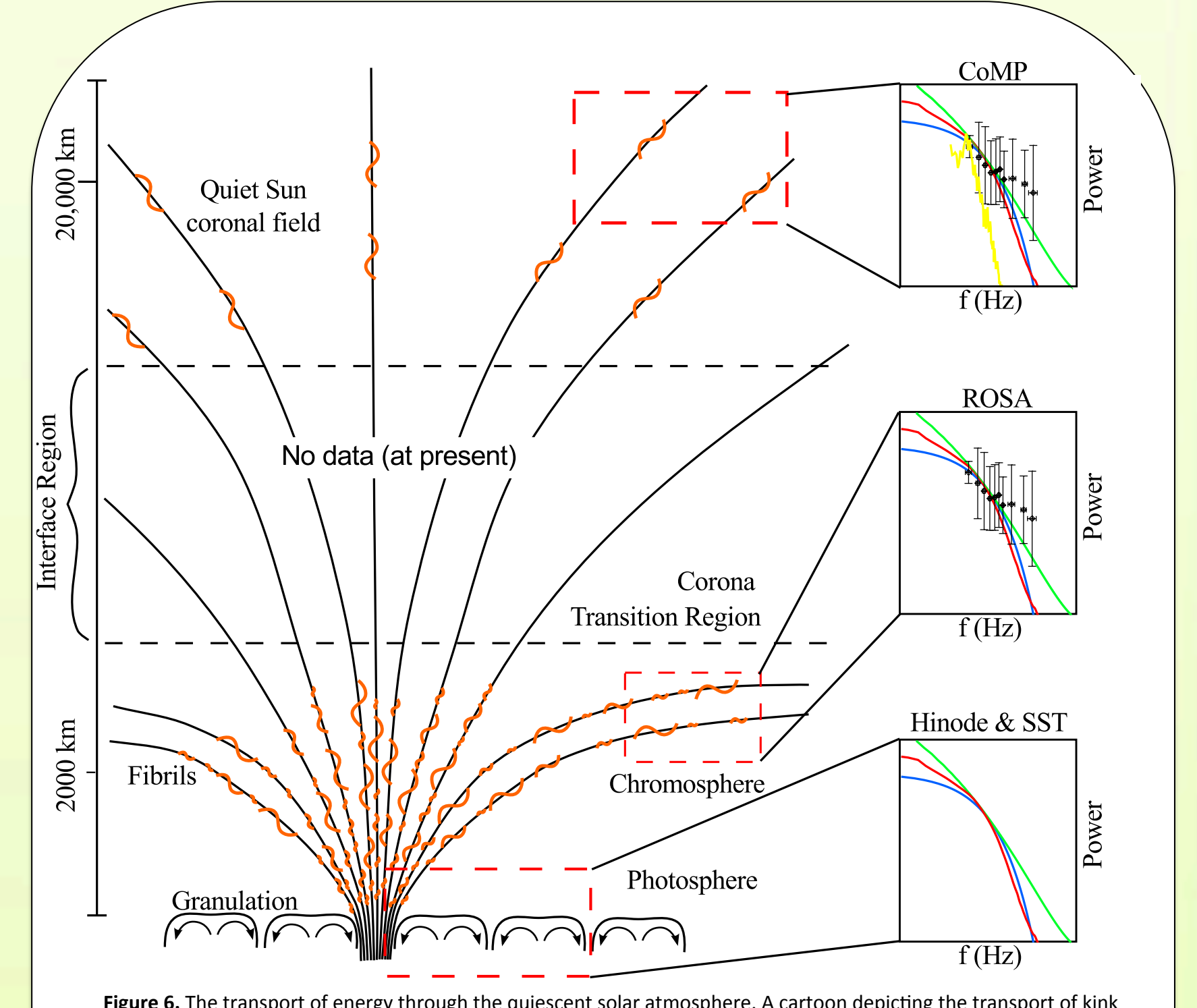


Figure 6. The transport of energy through the quiescent solar atmosphere. A cartoon depicting the transport of kink MHD wave energy through the solar atmosphere as implied by observational results. The kink MHD waves are assumed generated by the horizontal granular motions, which imparts a particular power spectrum on the waves. Kink MHD waves observed in the quiescent chromosphere demonstrate a similar power spectrum suggesting the granular motions have indeed excited them. The waves then enter a region that is difficult to observe with current solar instrumentation. We refer to this as the interface region and it consists of the Transition Region and low Corona. On reaching the upper Corona, CoMP measurements reveal that there has been a significant loss of higher frequency wave energy between the chromosphere and Corona. It could well be that the energy has been dissipated and is heating the solar atmosphere.

References

- [1] Osterbrock, ApJ, **134**, 347 (1961)
- [2] Narain & Ulmschneider, SSR, **757**, 453 (2002)
- [3] Cranmer & van Ballegoijen, ApJS, **171**, 265 (2005)
- [4] Matsumoto & Shibata, ApJ, **710**, 1857 (2010)
- [5] Antolin & Shibata, ApJ, **712**, 494 (2010)
- [6] De Pontieu et al., Science, **318**, 1574 (2007)
- [7] Morton et al., Nature Comms., **3**, 1315 (2012)
- [8] Tomczyk et al., Science, **317**, 1192 (2007)
- [9] McIntosh et al., Nature, **475**, 477 (2011)
- [10] Rutten, PTRS A, **370**, 3129 (2012)
- [11] Jess et al., Sol. Phys., **261**, 363 (2010)
- [12] Chitta et al., ApJ, **752**, 49 (2012)
- [13] Tomczyk & McIntosh, ApJ, **697**, 1384 (2009)
- [14] Morton et al., ApJ, **768**, 17 (2013)
- [15] Pereira et al., ApJ, **759**, 18 (2012)
- [16] Sekse et al., ApJ, **752**, 108 (2012)
- [17] Title et al., ApJ, **336**, 475 (1989)
- [18] Hillier et al., ApJ, Submitted (2013)
- [19] Verth et al., ApJ, **718**, L102 (2010)
- [20] Morton et al., ApJ, Submitted (2013)
- [21] De Moortel & Pascoe, ApJ, **746**, 31 (2012)
- [22] De Pontieu et al., ApJ, **752**, L12 (2012)